

# Electroaddressing of Cell Populations by Co-Deposition with Calcium Alginate Hydrogels

By Xiao-Wen Shi, Chen-Yu Tsao, Xiaohua Yang, Yi Liu, Peter Dykstra, Gary W. Rubloff, Reza Ghodssi, William E. Bentley, and Gregory F. Payne\*

Electroaddressing of biological components at specific device addresses is attractive because it enlists the capabilities of electronics to provide spatiotemporally controlled electrical signals. Here, the electrodeposition of calcium alginate hydrogels at specific electrode addresses is reported. The method employs the low pH generated at the anode to locally solubilize calcium ions from insoluble calcium carbonate. The solubilized  $\text{Ca}^{2+}$  can then bind alginate to induce this polysaccharide to undergo a localized sol-gel transition. Calcium alginate gel formation is shown to be spatially controlled in the normal and lateral dimensions. The deposition method is sufficiently benign that it can be used to entrap the bacteria *E. coli*. The entrapped cells are able to grow and respond to chemical inducers in their environment. Also, the entrapped cells can be liberated from the gel network by adding sodium citrate that can compete with alginate for  $\text{Ca}^{2+}$  binding. The capabilities of calcium alginate electrodeposition is illustrated by entrapping reporter cells that can recognize the quorum sensing autoinducer 2 (AI-2) signaling molecule. These reporter cells were observed to recognize and respond to AI-2 generated from an external bacterial population. Thus, calcium alginate electrodeposition provides a programmable method for the spatiotemporally controllable assembly of cell populations for cell-based biosensing and for studying cell-cell signaling.

## 1. Introduction

Recent advances in genomics and proteomics relied upon the development of methods for the spatially-selective coupling of nucleic acids and proteins to specific “address” locations. There is a similar interest in developing methods to assemble prokaryotic and eukaryotic cells at specific addresses for applications that range from fundamental study of cell-cell signaling to high

throughput screening and biosensing.<sup>[1–8]</sup> Current methods to assemble cells at specific addresses include; selective adhesion of cells onto patterned 2D surfaces,<sup>[9–11]</sup> photolithographic polymerization to entrap cells within 3D hydrogel networks,<sup>[12–18]</sup> and printing methods that deliver cell suspensions<sup>[19]</sup> or cell suspensions plus components that promote gel formation.<sup>[20–24]</sup> In addition, microfluidic devices have been designed that enable addressing or immobilization of cells within specific compartments.<sup>[25–29]</sup> Thus, a variety of novel methods have been developed to address and cultivate cells in array and microfluidic formats. Nevertheless, the search continues for simpler, generic, less expensive and more benign methods for cell addressing.

Traditionally, microbiologists have employed stimuli-responsive hydrogel-forming polysaccharides for cultivation and these polymers are also being extended to array and microfluidic formats. For instance, agar is a thermally-responsive polysaccharide that is routinely used in microbiology and recently, cell arrays have been printed onto<sup>[19]</sup> or within agar gels.<sup>[30,31]</sup> Alginate is an acidic polysaccharide that forms a gel in the presence of calcium ions. Calcium alginate gels are widely used to entrap and immobilize prokaryotes and eukaryotic cells, and recent research has extended the use of alginate to entrap cells and nanoparticles at the microscale.<sup>[32–35]</sup> In addition, cell- (or nanoparticle-) containing alginate beads,<sup>[36–41]</sup> bars,<sup>[42]</sup> tubes,<sup>[43]</sup> and multi-lamellar films<sup>[44]</sup> have been generated in microfluidic systems by controlling the contacting of streams

[\*] Prof. G. F. Payne, Dr. X.-W. Shi, Dr. C.-Y. Tsao, Dr. X. Yang, Dr. Y. Liu, Prof. W. E. Bentley  
Center for Biosystems Research  
University of Maryland Biotechnology Institute  
5115 Plant Sciences Building  
College Park, MD 20742 (USA)  
E-mail: payne@umbi.umd.edu  
Dr. C.-Y. Tsao, Prof. W. E. Bentley  
Fischell Department of Bioengineering  
University of Maryland  
College Park, MD 20742 (USA)

P. Dykstra, Prof. R. Ghodssi  
Department of Electrical and Computer Engineering  
University of Maryland  
College Park, MD 20742 (USA)  
Prof. G. W. Rubloff  
Department of Materials Science and Engineering  
University of Maryland  
College Park, MD 20742 (USA)  
Prof. G. W. Rubloff, Prof. R. Ghodssi  
Institute for Systems Research  
University of Maryland  
College Park, MD 20742 (USA)

DOI: 10.1002/adfm.200900026

containing alginate and calcium ions.<sup>[45]</sup> Hydrogel-forming polysaccharides may offer advantages for cultivation in array and microfluidic formats since they are familiar surfaces/matrices, they form gels under relatively mild conditions, and gel-formation is reversible allowing the entrapped hydrogel contents (e.g., cells) to be liberated intact.<sup>[3,42]</sup>

Here we report the electroaddressing of calcium alginate hydrogels and the ability to entrap viable cell populations within the electrodeposited films. Electroaddressing is particularly attractive for assembly because it employs the capabilities of microfabrication to create surfaces that can impose spatiotemporally-controlled electrical signals. To our knowledge, chitosan was the first hydrogel-forming polysaccharide to be electrodeposited.<sup>[46–48]</sup> Mechanistically, the pH-responsive chitosan is induced to undergo a sol–gel transition in response to the localized region of high pH established at the cathode surface.<sup>[49–51]</sup> Once electrodeposited at the cathode, the chitosan hydrogel film is stable in the absence of an applied voltage provided the pH is retained above its pKa (~6.5; chitosan re-dissolves at pH below its pKa). Recently, Cheong and Zhitomirsky<sup>[52]</sup> reported the anodic electrodeposition of alginic acid for the generation of composite films. They proposed a mechanism in which the localized low pH at the anode resulted in a neutralization of sodium alginate to alginic acid and neutralization of this polysaccharide resulted in gel formation. While this electrodeposition method is appropriate for the generation of composite materials, the low pH required to maintain the alginic acid gels may limit its use for culturing cells. Here, we report an alternative approach, the anodic electrodeposition of calcium alginate hydrogels, and we demonstrate its use for the electroaddressing of cell populations.

Scheme 1 illustrates the proposed mechanism for calcium alginate electrodeposition. The deposition solution contains soluble sodium alginate plus insoluble calcium carbonate (CaCO<sub>3</sub>). Electrochemical decomposition of water at the anode

leads to a pH gradient with a locally high proton concentration near the anode surface. This localized low pH triggers calcium release by the ‘solubilization’ reaction:



The acid-triggered Ca<sup>2+</sup>-solubilization reaction is further driven toward completion by the removal of CO<sub>2</sub> into the gas. The locally released Ca<sup>2+</sup> is then free to interact with the alginate chains<sup>[36,37,53]</sup> to generate the electrostatically-crosslinked hydrogel network.<sup>[54]</sup>

The goals of this work are to demonstrate calcium alginate electrodeposition and illustrate the potential utility of this method for the programmable and reversible assembly of cell populations at specific electrode addresses.

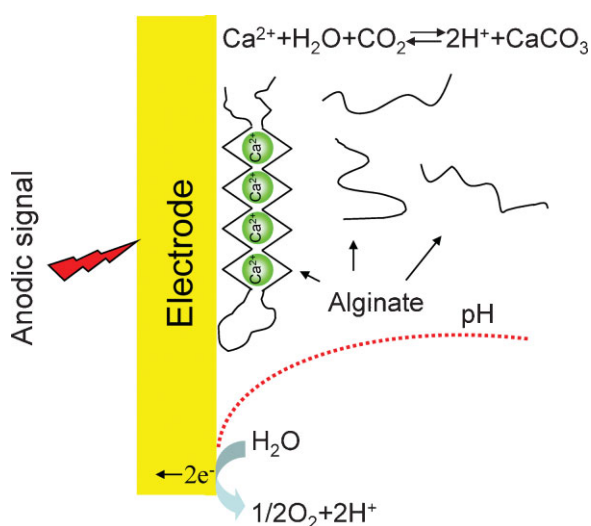
## 2. Results and Discussion

### 2.1. Electrodeposition of Calcium Alginate

Initial evidence for the electrodeposition of calcium alginate is provided in Figure 1. In this experiment CaCO<sub>3</sub> powder (10-μm particles; 0.25%) was blended into a sodium alginate (1.0%) solution and sonicated for 10 min. An ITO coated glass slide (2.5 cm × 1.0 cm) was partially immersed into this deposition solution and an anodic voltage was applied to achieve a current density of 3 A m<sup>-2</sup> (typical voltage is about 3.5 V) for 5 min (a platinum film served as the cathode). These conditions yield a thick deposit of calcium alginate. After electrodeposition, the ITO slide was removed from the solution and rinsed briefly with NaCl (0.1 M) solution, and then disconnected from the power supply. The photograph in Figure 1a shows the deposited film is relatively opaque (due to entrapped CaCO<sub>3</sub> particles) and contains several trapped bubbles (due to the generation of CO<sub>2</sub> and O<sub>2</sub>). A side view of this moist film is shown in Figure 1b, from which the thickness can be estimated to be about 1 mm. When electrodeposited films are sufficiently thick, they can be peeled from the substrate as illustrated in Figure 1c. To provide evidence that the film's opacity is due to entrapped CaCO<sub>3</sub> particles we immersed the film in acid (0.1 M HCl) for 10 min. Figure 1d shows that the acid-treated film is transparent due to the solubilization of the CaCO<sub>3</sub>.

To demonstrate that the electrodeposition of calcium alginate can be controlled, we electrodeposited films for various times. After deposition, the films were air dried at room temperature for 24 h and the film thickness was measured by profilometry. Figure 1e shows an increase in film thickness with deposition time. These results demonstrate that calcium alginate gels can be controllably electrodeposited at the anode.

The spatial selectivity of calcium alginate electrodeposition was next examined using the chip shown in Figure 2a, which possesses two patterned gold electrodes (0.25 mm and 1 mm). To facilitate visualization we added fluorescently labeled microparticles (1 μm; 0.1%) into alginate–CaCO<sub>3</sub> suspension (1% alginate; 0.25% CaCO<sub>3</sub>). Deposition was performed by connecting both electrodes to the power supply and applying an anodic



**Scheme 1.** Mechanism for calcium alginate electrodeposition. The pH gradient at the anode triggers calcium release from insoluble CaCO<sub>3</sub> and this induces the localized gelation of calcium alginate at the anode surface.

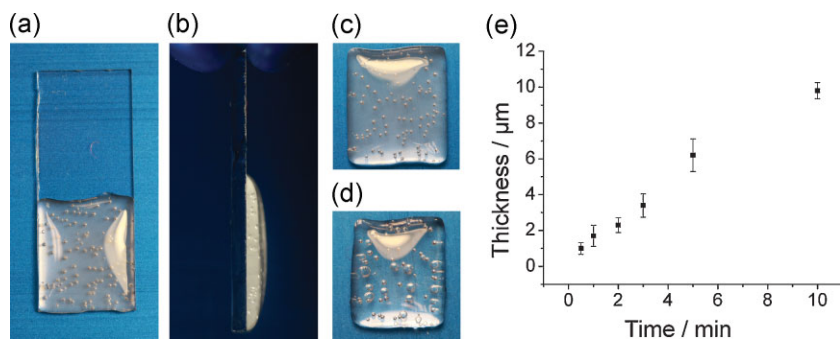


**Figure 1.** Electrodeposition of calcium alginate gel on an ITO-coated glass slide. a) Front and b) side views of a gel electrodeposited for 5 min at a current density of  $3 \text{ A m}^{-2}$ . c) Calcium alginate hydrogel peeled from the slide. d) Hydrogel after treatment with  $0.1 \text{ M HCl}$  to solubilize entrapped  $\text{CaCO}_3$ . e) Thickness of dried calcium alginate films that had been electrodeposited for varying times.

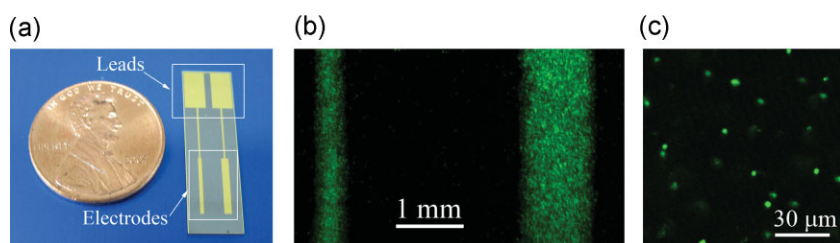


**Figure 2.** Spatial selectivity of calcium alginate electrodeposition on a patterned chip. a) The chip is a silicon wafer with two patterned gold electrodes ( $0.25 \text{ mm}$  and  $1 \text{ mm}$  width). b) Fluorescence photomicrograph of electrodeposited calcium alginate gels with entrapped fluorescent microparticles. c) Confocal fluorescence image from the middle depth of the alginate gel with entrapped fluorescent microparticles.

voltage at  $1 \text{ A m}^{-2}$  for 2 min (a platinum film served as the cathode). The fluorescence photomicrograph in Figure 2b shows that fluorescence is observed on both electrodes and that fluorescence is spatially confined in the lateral dimensions to the electrode surfaces. The graininess of the fluorescence in Figure 2b suggests that the microparticles are entrapped as individual particles. To support this conclusion, we imaged the internal region of the deposited film using confocal fluorescence microscopy. Figure 2c shows a fluorescence image from the middle depth of the alginate film and indicates that the microparticles are dispersed and entrapped throughout the gel network. The results in Figure 2 demonstrate that calcium alginate electrodeposition is spatially selective in the lateral dimension.

## 2.2. Entrap, Grow, Induce, and Liberate *E. coli*

We examined the potential for co-depositing and entrapping *E. coli* cells within electrodeposited calcium alginate gels. The cells for inoculation were initially cultured in LB medium to an  $\text{OD}_{600}$  of 1.0 and then diluted 10-fold in a suspension of alginate and  $\text{CaCO}_3$  (final concentrations;  $0.9\%$  alginate and  $0.23\%$   $\text{CaCO}_3$ ). An ITO-coated slide was

partially immersed in this suspension and an anodic voltage was applied to a current density of  $3 \text{ A m}^{-2}$  for 2 min. After electrodeposition, the resulting gel was washed with  $1.0\%$  NaCl and hardened by immersion in  $1.0\%$   $\text{CaCl}_2$  solution for 30 min at  $4^\circ\text{C}$ . The slide with the entrapped cells was then incubated with LB medium at  $37^\circ\text{C}$ , and the optical density was intermittently measured. The growth curve in Figure 3a shows a steady increase in optical density for the inoculated gels, while a control film electrodeposited without cells shows no change in optical density. The photographs of the inoculated and control alginate films in Figure 3b show an obvious difference in optical density between these hydrogel films.

The bright field image in Figure 3c was obtained after incubating the cells for 7 h in the alginate gel. This image indicates that cell growth is accompanied by the appearance of  $20\text{--}30\text{-}\mu\text{m}$  colonies. Presumably the colonies are the result of cell division that is spatially confined to specific regions of the alginate gels. No colonies were observed in the inoculum or immediately after co-depositing cells within the alginate gel (images not shown). This observation would suggest that the bacterial cells are entrapped and unable to freely move through the calcium alginate network (i.e., daughter cells are retained near the mother). The results in Figure 3

indicate that *E. coli* can be co-deposited and entrapped within calcium alginate gels, and that co-deposited cells remain viable and are able to grow.

Next we examined whether co-deposited *E. coli* cells entrapped within an alginate gel could be induced to express a foreign protein in response to an externally-added inducer. In particular, we used recombinant cells that express green fluorescent protein (GFP) in response to IPTG induction. Using methods described above, the cells were co-deposited with alginate and  $\text{CaCO}_3$ , hardened with  $\text{CaCl}_2$ , and then incubated in LB medium at  $37^\circ\text{C}$  for 2 h. After this initial incubation, IPTG ( $1 \text{ mM}$  final concentration) was added and the fluorescence of the gel was

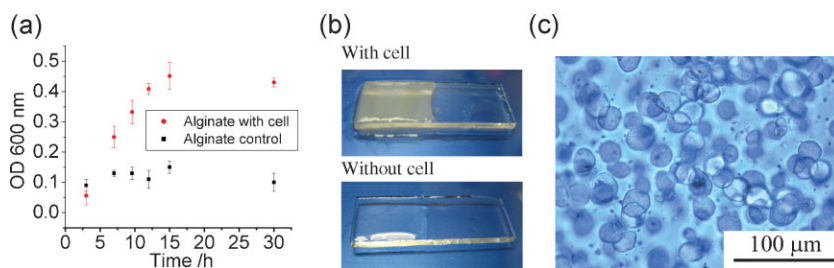


**Figure 3.** Growth of entrapped *E. coli* cells co-deposited with the calcium alginate hydrogel. a) Growth curve as measured by optical density for cells incubated at  $37^\circ\text{C}$ . b) The photographs of the inoculated and control alginate films after incubation for 24 h. c) Bright field image of cell colonies ( $20\text{--}30\text{-}\mu\text{m}$ ) after incubation for 7 hours in the alginate gel.

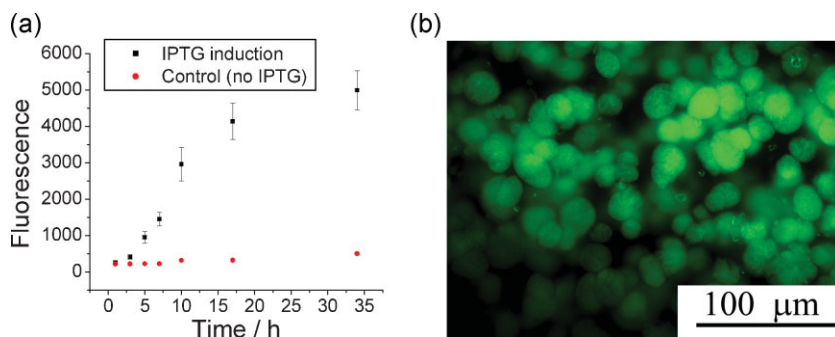


**Figure 4.** Induction of entrapped *E. coli* cells to express the green fluorescence protein (GFP). a) Time course for the appearance of fluorescence after IPTG induction. b) Fluorescence photomicrograph of induced *E. coli* cells entrapped within the alginate gel.

monitored. Figure 4a shows that 3 h after adding IPTG, the fluorescence began to increase and a nearly linear increase in fluorescence was observed until 17 h. The control cells that had been co-deposited but not induced by IPTG showed little change in fluorescence during incubation. At the end of the experiment the induced cells were imaged using a fluorescence photomicroscope. The image in Figure 4b shows that the fluorescence for the induced cells appears to be spatially confined to small regions (i.e., colonies) within the alginate gel. This spatial confinement of induced cells within the alginate network is consistent with observations in Figure 3c. The results in Figure 4 demonstrate that entrapped cells can respond to their environment (i.e., they can be induced).

Potentially, electroaddressing by calcium alginate electrodeposition provides a simple means to perform multiplexed cell-based biosensing. To illustrate this capability, we performed the experiment outlined in Figure 5a in which two different populations of *E. coli* were electrodeposited and entrapped at

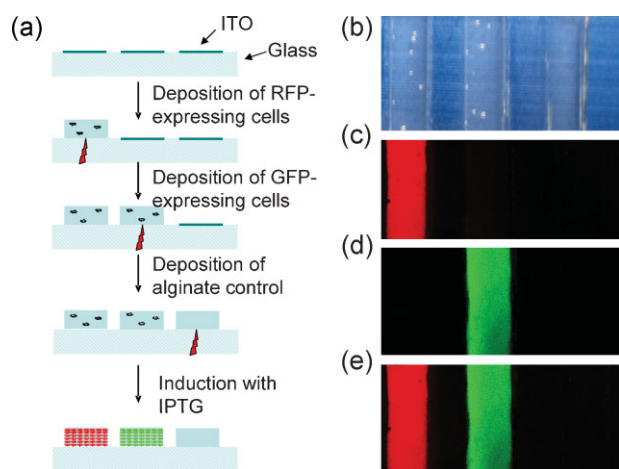


**Figure 5.** Electroaddressing of two different *E. coli* populations to patterned ITO electrodes (2-mm wide). a) Schematic illustrating the sequential co-deposition of cells that express RFP (left electrode) and GFP (middle electrode) followed by the deposition of a control alginate gel (right electrode). b) Photograph of patterned slide after sequential deposition. c, d) Fluorescence photomicrographs of the patterned slide after IPTG induction using red or green filters. e) Composite image of red and green fluorescence.

separate electrode addresses of the patterned ITO-coated slide in Figure 5b. We first co-deposited RFP-expressing *E. coli* by immersing the patterned slide in the cell–alginate–CaCO<sub>3</sub> suspension and biasing the left-most electrode ( $3 \text{ A m}^{-2}$  for 2 min). After washing with NaCl, we next co-deposited GFP-expressing *E. coli* by immersing the slide in a second cell–alginate–CaCO<sub>3</sub> suspension and biasing the middle electrode. After rinsing with NaCl, calcium alginate (without cells) was electrodeposited at the right-most electrode (the control electrode). This slide was incubated in LB medium for 2 h after which the IPTG inducer was added and then the slide was further incubated overnight for an additional 16 h.

The two images in Figure 5c and 5d are fluorescence photomicrographs using individual red and green filters while the image in Figure 5e is a composite image. These images indicate that RFP-expressing cells are selectively confined on the left electrode address while GFP-expressing cells are selectively confined on the middle address. No fluorescence is visible on the control electrode. This result indicates that there is little cross talk between the three electrodes. Specifically, the cells are electrodeposited at their specific address and do not substantially migrate to other addresses during the 18 h experiment.

One advantage of using (bio)polymers that can undergo a reversible sol–gel transition is that the entrapped cells can be liberated from the matrix in response to external stimuli. For the case of calcium alginate, the hydrogel network can be disrupted by the addition of chemicals that preferentially bind calcium.<sup>[3,42]</sup> To demonstrate this ability, we co-deposited recombinant *E. coli* onto a patterned ITO electrode (10 mm × 2 mm) and induced these cells (with IPTG) to express GFP. After overnight incubation, the slide was examined and the photomicrograph of Figure 6a shows strong fluorescence at this electrode address. To liberate the alginate-entrapped cells, we immersed the slide in PBS buffer (100 mM; pH 7.4) containing sodium citrate

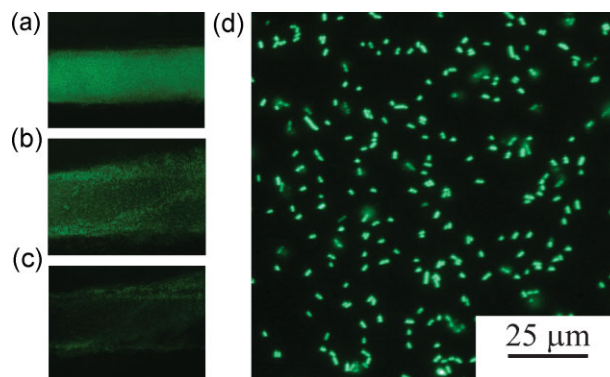


**Figure 6.** Liberation of calcium alginate entrapped cells using sodium citrate. a) Alginate entrapped, GFP-expressing *E. coli* cells before adding citrate. b) Partial dissolution of calcium alginate gel after 2 min incubation with citrate. c) Nearly complete dissolution of alginate gel after 5 min incubation with citrate. d) Fluorescence image of liberated cells.

(500 mM) and applied gentle shaking. As illustrated in Figure 6b, the alginate gel began dissolving within 2 min and dissolution was nearly complete in 5 min (Figure 6c). Figure 6d shows that the liberated *E. coli* appear as individual cells (and not multicellular colonies). These results demonstrate that the alginate-entrapped cells can be liberated intact by the addition of sodium citrate that can bind calcium.

### 2.3. Signaling Between Entrapped and Suspended Cells

In a final set of experiments we examined the ability of the alginate entrapped cells to communicate with a cell population outside the alginate network. Specifically, we tested the cell–cell communication system associated with bacterial quorum sensing. This system is mediated by small signaling molecules known as autoinducers<sup>[55–59]</sup> that are synthesized and secreted by bacteria, and later “sensed” by neighboring cells of the same or different species depending on the particular niche. Quorum sensing leads to changes in gene expression and cell phenotype, with a transition from single cell behavior to coordinated multicellular behavior. For instance, autoinducers have been implicated in controlling the virulence of the pathogenic *E. coli* O157:H7.<sup>[60,61]</sup> In our studies, we examined MDAI2 *E. coli* which was unable to synthesize autoinducer 2 (AI-2) because we deleted its terminal synthase gene, *luxS*. We also employed a novel reporter strain, MDAI2 (pCT6+pET-GFPuv), which was engineered to respond to AI-2 by expressing GFP.

In our initial experiment we electrodeposited MDAI2 (pCT6+pET-GFPuv) reporter cells in the calcium alginate gel. These entrapped cells were then incubated in 2 mL LB medium containing 200  $\mu$ L of a solution obtained from the *in vitro* synthesis of AI-2. After incubation at 26 °C for 16 h, the entrapped cells were imaged using fluorescence photomicroscopy. Figure 7a shows considerable GFP fluorescence for these entrapped reporter cells which indicates that they are able to respond to the added AI-2. One control in Figure 7b is entrapped MDAI2 (pCT6+pET-GFPuv) reporter cells incubated with LB that lacked AI-2 addition. As expected, no GFP fluorescence is observed in the image for this control. A second control in Figure 7c is entrapped MDAI2 cells that are neither able to synthesize AI-2 nor respond to AI-2 by expressing GFP. As expected, incubation of these entrapped cells with AI-2 does not lead to the induction of GFP as evidenced from the image in Figure 7c. The results in Figure 7 indicate that MDAI2 (pCT6+pET-GFPuv) is a useful reporter cell

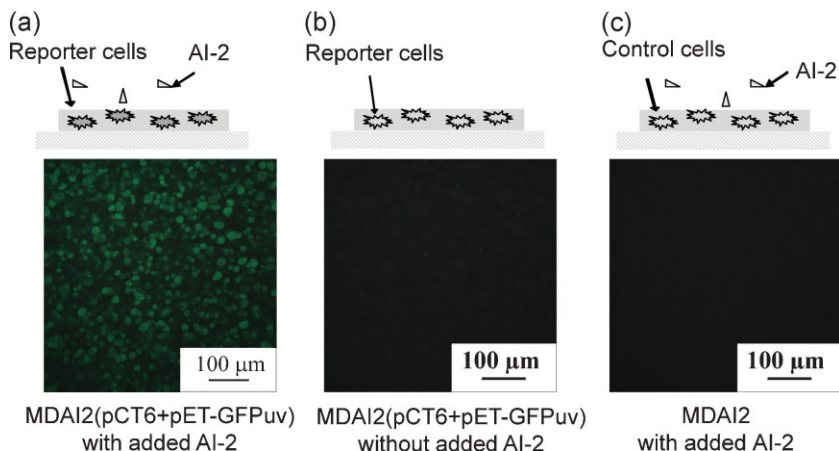


**Figure 7.** Alginate entrapped reporter cells that respond to autoinducer 2 (AI-2) by expressing GFP. a) Fluorescence image of alginate-entrapped reporter cells (MDAI2(pCT6+pET-GFPuv)) incubated with added AI-2. b) Control of alginate-entrapped reporter cells incubated in the absence of AI-2. c) Control of alginate-entrapped non-reporter cells (MDAI2) incubated in the presence of AI-2.

line that can detect externally added AI-2 and respond by expressing GFP.

In our final experiment, we electrodeposited MDAI2 (pCT6+pET-GFPuv) reporter cells in the calcium alginate gel. These entrapped cells were then incubated in 2 mL LB medium and a second culture, BL21 *E. coli*, was inoculated into the liquid phase (2  $\mu$ L of BL21 OD<sub>600</sub> = 3.9). The liquid phase BL21 *E. coli* can produce and secrete AI-2 and should be able to signal to the entrapped reporter cells that can detect and respond to AI-2. These co-cultures were incubated at 26 °C for 16 h. The fluorescence photomicrograph in Figure 8a shows that the entrapped reporter cells became fluorescent in this co-culture. The first control in Figure 8b is a co-culture of entrapped MDAI2

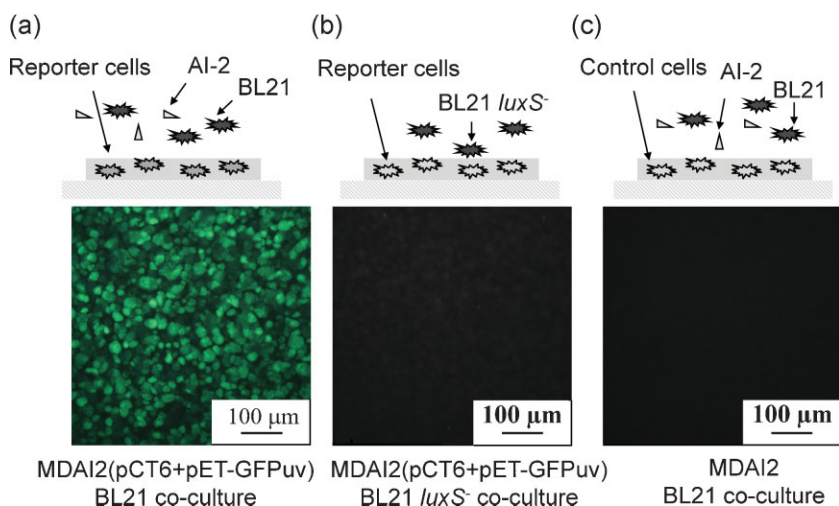


**Figure 8.** Signaling between alginate-entrapped reporter cells and an external cell population. a) Fluorescence image of alginate-entrapped reporter cells (MDAI2(pCT6+pET-GFPuv)) co-cultured with BL21 *E. coli* that can synthesize and secrete AI-2. b) Control of alginate-entrapped reporter cells co-cultured with BL21 *luxS*<sup>-</sup> *E. coli* that lack the ability to synthesize and secrete AI-2. c) Control of alginate-entrapped non-reporter cells (MDAI2) co-cultured with BL21 *E. coli*.

(pCT6+pET-GFPuv) reporter cells with a BL21 *luxS* knockout strain in the liquid phase. This BL21 *luxS* knockout strain is unable to synthesize AI-2 and thus should be unable to generate the quorum sensing signaling molecule to induce GFP expression in the entrapped reporter cells. As expected, the fluorescence photomicrograph in Figure 8b shows no fluorescence for the entrapped reporter cells in this control. The second control in Figure 8c is a co-culture of entrapped MDAI2 (unable to synthesize AI-2 or express GFP in response to AI-2) and liquid phase BL21 which can synthesize AI-2. As expected, Figure 8c shows no fluorescence in this control. The results in Figures 7 and 8 indicate that the entrapped reporter cells are capable of reporting the presence of the AI-2 signaling molecule.

### 3. Conclusions

We report the electrodeposition of calcium alginate hydrogel films in response to an anodic signal (i.e., a pH decrease) that triggers a localized release of calcium. Electrodeposition is achieved under sufficiently mild conditions that bacterial cells can be entrapped without destroying viability. The entrapped cells were observed to grow and respond to their environment (i.e., they could be induced). In addition, because gel formation is reversible, the entrapped cells can be liberated from the gels by the use of agents (i.e., citrate) that out-compete alginate for calcium binding.<sup>[3,42]</sup> Potentially, this work is significant because it provides a reagentless method to electroaddress and entrap cells within a benign calcium alginate matrix. Calcium alginate hydrogels are routinely used for microbiological cultivation and are often considered for tissue engineering scaffolds.<sup>[62,63]</sup> We anticipate that this simple, rapid, and benign method for the programmable electroaddressing of cell populations could have broad applications for cell based biosensing in array or microfluidic formats.

The results with the quorum sensing reporter cells indicate that the alginate entrapped cells can “communicate” with external cell populations. Co-deposition with calcium alginate provides a convenient means to spatially segregate one population of cells (e.g., reporter cells) while allowing communication with co-cultured populations through diffusible signaling molecules. Thus, calcium alginate electrodeposition may provide a convenient experimental method for studying cell-cell signaling.

### 4. Experimental

The following materials were purchased from Sigma-Aldrich: sodium alginate from *Macrocystis Pyrifera* (medium viscosity), calcium carbonate powder (10  $\mu\text{m}$ ),  $\text{CaCl}_2$  pellets, phosphate buffered saline (PBS, pH 7.4), isopropyl  $\beta$ -D-1-thiogalactopyranoside (IPTG), FITC-labeled microparticles based on melamine resin (1  $\mu\text{m}$ ), and indium tin oxide (ITO)-coated glass slides (surface resistivity 8–12  $\Omega \text{ sq}^{-1}$ ). Luria-Bertani (LB) medium was purchased from Acros. Silicon wafers were patterned with gold using standard photolithographic methods as previously described [64].

Initial electrodeposition studies were performed using either ITO-coated slides or patterned silicon chips as anodes, and a platinum film as the cathode. The deposition solution was prepared by suspending  $\text{CaCO}_3$  powder (10- $\mu\text{m}$  particles; 0.25%) into a sodium alginate (1.0%) and sonicating for 10 min. For deposition with ITO-coated glass slides, the

slides were partially immersed in the deposition solution and an anodic voltage was applied to achieve a current density of 3  $\text{A m}^{-2}$  (the deposition time was varied). To measure thickness of the electrodeposited calcium alginate, the ITO-coated slide was dried in air for 24 h and measured using a profilometer (Alpha-step 500 Surface Profiler, TENCOR Instruments). To examine the spatial selectivity for electrodeposition, FITC-labeled microparticles (1- $\mu\text{m}$  particles, 0.1%) were blended into the deposition solution and deposition was performed using a chip with patterned gold electrodes. For deposition, the chip was partially immersed in the deposition solution and an anodic voltage was applied for 2 min to achieve 1  $\text{A m}^{-2}$  (a lower current density was used to prevent destruction of the gold electrodes). The microparticle-containing films deposited on the patterned electrodes were imaged using a Leica fluorescence microscope (MZFL III) connected with a digital camera (spot 32, Diagnostic Instrument).

Several *E. coli* strains were examined in this study. Strains that express green fluorescent protein (GFP) and red fluorescent protein (RFP) in response to IPTG induction were described elsewhere [65]. These strains were cultured in LB medium containing 50  $\mu\text{g mL}^{-1}$  kanamycin and 34  $\mu\text{g mL}^{-1}$  chloramphenicol. Several strains were examined that have altered abilities to recognize and respond to the quorum sensing autoinducer-2 (AI-2) (molecular biological details of these constructs will be published separately). Briefly, *E. coli* MDAI2 is a *luxS* knockout strain that is unable to synthesize AI-2 [66]. MDAI2 (pCT6+pET-GFPuv) is obtained by transforming MDAI2 with two plasmids to enable this strain to respond to exogenously-added AI-2 by expressing GFP. *E. coli* BL21 (Novagen) was used in co-culture experiments and this strain can produce endogenous AI-2. The *luxS* knockout mutant, *E. coli* BL21 *luxS* [67], is unable to produce AI-2.

In vitro AI-2 was synthesized using a procedure described previously [68,69]. Briefly, 1 mM S-adenosylhomocysteine was reacted with the two purified enzymes His<sub>6</sub>-Pfs and His<sub>6</sub>-LuxS in 50 mM Tris-HCl (pH 7.8) at 37 °C for 4h. The conversion was estimated to be about 60% based on the quantification of free thiols by DTNB (5,5'-Dithiobis (2-nitrobenzoic acid) [67].

To co-deposit the *E. coli* strains, the cells were initially cultured in LB medium to an optical density at 600 nm (OD<sub>600</sub>) of 1.0 and then diluted 10-fold into an alginate- $\text{CaCO}_3$  suspension that had been previously autoclaved. ITO-coated glass slides that had been sterilized with ethanol were partially immersed into the cell–alginate– $\text{CaCO}_3$  deposition solution and an anodic voltage was applied for 2 min to achieve a current density of 3  $\text{A m}^{-2}$ . After deposition, the slides were washed with 1.0% NaCl and the alginate gel was hardened in 1.0%  $\text{CaCl}_2$  solution for 30 min at 4 °C. The alginate entrapped cells were incubated in 2 mL LB medium and various additions were made as described in the text. Various methods were used to examine the entrapped cells: optical density was measured using a spectrophotometer (DU640 Beckman); fluorescence was quantified using a fluorescence microplate reader for alginate films that had been peeled from the slides (SpectraMax5, Molecular Devices); bright field images were obtained using a confocal microscope (IX81-DSU, Olympus); fluorescence images were obtained using a fluorescence microscope (BX-60, Olympus or MZFL III Leica) and a scanning confocal laser microscope (Zeiss LSM 510 with an Ar laser at 488 nm).

### Acknowledgements

The authors gratefully acknowledge financial support from the R.W. Deutsch Foundation, the National Science Foundation (NSF; EFRI-0735987), and the Department of Defense, Defense Threat Reduction Agency (W91B9480520121).

Received: January 7, 2009  
Published online: May 14, 2009

[1] T. H. Park, M. L. Shuler, *Biotechnol. Prog.* **2003**, *19*, 243.

[2] T. Elad, J. H. Lee, S. Belkin, M. B. Gu, *Microb. Biotechnol.* **2008**, *1*, 137.

- [3] R. M. Johann, *Anal. Bioanal. Chem.* **2006**, *385*, 408.
- [4] K. Yagi, *Appl. Microbiol. Biotechnol.* **2007**, *73*, 1251.
- [5] H. Andersson, A. van den Berg, *Sens. Actuator B-Chem.* **2003**, *92*, 315.
- [6] H. Nakamura, M. Shimomura-Shimizu, I. Karube, *Biosensing for the 21st Century*, Vol. 109, Springer-Verlag Berlin, Berlin **2008**, 351.
- [7] A. A. Iniesta, P. T. McGrath, A. Reisenauer, H. H. McAdams, L. Shapiro, *Proc. Natl. Acad. Sci. USA* **2006**, *103*, 10935.
- [8] M. Y. Lee, R. A. Kumar, S. M. Sukumaran, M. G. Hogg, D. S. Clark, J. S. Dordick, *Proc. Natl. Acad. Sci. USA* **2008**, *105*, 59.
- [9] Y. C. Lu, Y. S. Chuang, Y. Y. Chen, A. C. Shu, H. Y. Hsu, H. Y. Chang, T. R. Yew, *Biosens. Bioelectron.* **2008**, *23*, 1856.
- [10] O. Laczka, E. Baldrich, F. X. Munoz, F. J. del Campo, *Anal. Chem.* **2008**, *80*, 7239.
- [11] S. Da Silva, L. Grosjean, N. Ternan, P. Mailley, T. Livache, S. Cosnier, *Bioelectrochemistry* **2004**, *63*, 297.
- [12] A. Revzin, R. J. Russell, V. K. Yadavalli, W.-G. Koh, C. Deister, D. D. Hile, M. B. Mellott, M. V. Pishko, *Langmuir* **2001**, *17*, 5440.
- [13] W. G. Koh, A. Revzin, M. V. Pishko, *Langmuir* **2002**, *18*, 2459.
- [14] W.-G. Koh, M. Pishko, *Langmuir* **2003**, *19*, 10310.
- [15] W.-G. Koh, L. J. Itle, M. V. Pishko, *Anal. Chem.* **2003**, *75*, 5783.
- [16] J. Heo, K. J. Thomas, G. H. Seong, R. M. Crooks, *Anal. Chem.* **2003**, *75*, 22.
- [17] D. R. Albrecht, V. L. Tsang, R. L. Sah, S. N. Bhatia, *Lab Chip* **2005**, *5*, 111.
- [18] Z. H. Nie, E. Kumacheva, *Nat. Mater.* **2008**, *7*, 277.
- [19] T. Xu, S. Petridou, E. H. Lee, E. A. Roth, N. R. Vyavahare, J. J. Hickman, T. Boland, *Biotechnol. Bioeng.* **2004**, *85*, 29.
- [20] M. C. Flickinger, J. L. Schottel, D. R. Bond, A. Aksan, L. E. Scriven, *Biotechnol. Prog.* **2007**, *23*, 2.
- [21] O. K. Lyngberg, V. Thiagarajan, D. J. Stemke, J. L. Schottel, L. E. Scriven, M. C. Flickinger, *Biotechnol. Bioeng.* **1999**, *62*, 44.
- [22] K. L. Swope, M. C. Flickinger, *Biotechnol. Bioeng.* **1996**, *52*, 340.
- [23] K. L. Swope, M. C. Flickinger, *Biotechnol. Bioeng.* **1996**, *51*, 360.
- [24] D. O. Fesenko, T. V. Nasedkina, D. V. Prokopenko, A. D. Mirzabekov, *Biosens. Bioelectron.* **2005**, *20*, 1860.
- [25] P. J. Lee, P. J. Hung, V. M. Rao, L. P. Lee, *Biotechnol. Bioeng.* **2006**, *94*, 5.
- [26] P. J. Hung, P. J. Lee, P. Sabounchi, N. Aghdam, R. Lin, L. P. Lee, *Lab Chip* **2005**, *5*, 44.
- [27] P. J. Hung, P. J. Lee, P. Sabounchi, R. Lin, L. P. Lee, *Biotechnol. Bioeng.* **2005**, *89*, 1.
- [28] M. Yang, C. W. Li, J. Yang, *Anal. Chem.* **2002**, *74*, 3991.
- [29] J. Yang, C. W. Li, M. Yang, *Lab Chip* **2004**, *4*, 53.
- [30] J. H. Lee, R. J. Mitchell, B. C. Kim, D. C. Cullen, M. B. Gu, *Biosens. Bioelectron.* **2005**, *21*, 500.
- [31] J. H. Lee, C. H. Youn, B. C. Kim, M. B. Gu, *Biosens. Bioelectron.* **2007**, *22*, 2223.
- [32] C. Qiu, M. Chen, H. Yan, H. K. Wu, *Adv. Mater.* **2007**, *19*, 1603.
- [33] D. Hardison, H. U. Deepthike, W. Senevirathna, T. Pathirathne, M. Wells, *J. Mater. Chem.* **2008**, *18*, 5368.
- [34] T. Sakaguchi, Y. Morioka, M. Yamasaki, J. Iwanaga, K. Beppu, H. Maeda, Y. Morita, E. Tamiya, *Biosens. Bioelectron.* **2007**, *22*, 1345.
- [35] L. Grossin, D. Cortial, B. Saulnier, O. Félix, A. Chassepot, G. Decher, P. Netter, P. Schaaf, P. Gillet, D. Mainard, J.-C. Voegel, N. Benkirane-Jessel, *Adv. Mater.* **2009**, *21*, 650.
- [36] W. H. Tan, S. Takeuchi, *Adv. Mater.* **2007**, *19*, 2696.
- [37] H. Zhang, E. Tumarkin, R. M. A. Sullan, G. C. Walker, E. Kumacheva, *Macromol. Rapid Commun.* **2007**, *28*, 527.
- [38] V. L. Workman, S. B. Dunnett, P. Kille, D. D. Palmer, *Macromol. Rapid Commun.* **2008**, *29*, 165.
- [39] S. Sugiura, T. Oda, Y. Izumida, Y. Aoyagi, M. Satake, A. Ochiai, N. Ohkohchi, M. Nakajima, *Biomaterials* **2005**, *26*, 3327.
- [40] K. S. Huang, T. H. Lai, Y. C. Lin, *Lab Chip* **2006**, *6*, 954.
- [41] L. Capretto, S. Mazzitelli, C. Balestra, A. Tosi, C. Nastruzzi, *Lab Chip* **2008**, *8*, 617.
- [42] T. Braschler, R. Johann, M. Heule, L. Metref, P. Renaud, *Lab Chip* **2005**, *5*, 553.
- [43] S. Sugiura, T. Oda, Y. Aoyagi, M. Satake, N. Ohkohchi, M. Nakajima, *Lab Chip* **2008**, *8*, 1255.
- [44] R. M. Johann, P. Renaud, *Biointerphases* **2007**, *2*, 73.
- [45] K. Liu, H.-J. Ding, J. Liu, Y. Chen, X.-Z. Zhao, *Langmuir* **2006**, *22*, 9453.
- [46] L. Q. Wu, A. P. Gadre, H. M. Yi, M. J. Kastantin, G. W. Rubloff, W. E. Bentley, G. F. Payne, R. Ghodssi, *Langmuir* **2002**, *18*, 8620.
- [47] X. Pang, I. Zhitomirsky, *Mater. Chem. Phys.* **2005**, *94*, 245.
- [48] X. L. Luo, J. J. Xu, Y. Du, H. Y. Chen, *Anal. Biochem.* **2004**, *334*, 284.
- [49] R. Fernandes, L. Q. Wu, T. H. Chen, H. M. Yi, G. W. Rubloff, R. Ghodssi, W. E. Bentley, G. F. Payne, *Langmuir* **2003**, *19*, 4058.
- [50] R. A. Zangmeister, J. J. Park, G. W. Rubloff, M. J. Tarlov, *Electrochim. Acta* **2006**, *51*, 5324.
- [51] X. Pang, I. Zhitomirsky, *Mater. Charact.* **2007**, *58*, 339.
- [52] M. Cheong, I. Zhitomirsky, *Colloid Surf. A* **2008**, *328*, 73.
- [53] A. W. J. Chan, I. Mazeaud, T. Becker, R. J. Neufeld, *Enzyme Microb. Technol.* **2006**, *38*, 265.
- [54] P. Sikorski, F. Mo, G. Skjak-Brk, B. T. Stokke, *Biomacromolecules* **2007**, *8*, 2098.
- [55] S. Hooshangi, W. E. Bentley, *Curr. Opin. Biotechnol.* **2008**, *19*, 550.
- [56] L. Wang, Y. Hashimoto, C. Y. Tsao, J. J. Valdes, W. E. Bentley, *J. Bacteriol.* **2005**, *187*, 2066.
- [57] M. E. Taga, S. T. Miller, B. L. Bassler, *Mol. Microbiol.* **2003**, *50*, 1411.
- [58] D. T. Hughes, V. Sperandio, *Nat. Rev. Microbiol.* **2008**, *6*, 111.
- [59] C. Fuqua, E. P. Greenberg, *Proc. Natl. Acad. Sci. U S A* **1998**, *95*, 6571.
- [60] V. Sperandio, A. G. Torres, B. Jarvis, J. P. Nataro, J. B. Kaper, *Proc. Natl. Acad. Sci. USA* **2003**, *100*, 8951.
- [61] S. K. Anand, M. W. Griffiths, *Int. J. Food Microbiol.* **2003**, *85*, 1.
- [62] M. Rinaudo, *Polym. Int.* **2008**, *57*, 397.
- [63] J. M. Dang, K. W. Leong, *Adv. Drug Deliv. Rev.* **2006**, *58*, 487.
- [64] L.-Q. Wu, H. Yi, S. Li, G. W. Rubloff, W. E. Bentley, R. Ghodssi, G. F. Payne, *Langmuir* **2003**, *19*, 519.
- [65] X. Yang, X.-W. Shi, Y. Liu, W. E. Bentley, G. F. Payne, *Langmuir* **2009**, *25*, 338.
- [66] M. P. DeLisa, J. J. Valdes, W. E. Bentley, *J. Bacteriol.* **2001**, *183*, 2918.
- [67] R. Fernandes, W. E. Bentley, *Biotechnol. Bioeng.* **2008**, *102*, 390.
- [68] A. F. Gonzalez Barrios, R. Zuo, Y. Hashimoto, L. Yang, W. E. Bentley, T. K. Wood, *J. Bacteriol.* **2006**, *188*, 305.
- [69] R. Fernandes, C. Y. Tsao, Y. Hashimoto, L. Wang, T. K. Wood, G. F. Payne, W. E. Bentley, *Metab. Eng.* **2007**, *9*, 228.